URTeC: 3724091

Using Geochemical Production Allocation to Calibrate Hydraulic Fracture and Reservoir Simulation Models: A Permian Basin Case Study

Magdalene Albrecht*[1], Shannon Borchardt[1], Mark McClure[2], 1. SM Energy, 2. ResFrac Corporation.

This paper was prepared for presentation at the Unconventional Resources Technology Conference held in Houston, Texas, USA, 20-22 June 2022.

Abstract

This paper demonstrates how geochemical production allocations can be used to calibrate reservoir simulation models and improve the optimization of well spacing and hydraulic fracture design in unconventional assets. Geochemical analyses provide quantitative assessments of flow by layer over time. This allows numerical models to be fine-tuned to realistically capture the productive fracture height for wells landed in different stratigraphic layers. Model calibration that relies on production and pressure history alone often fails to uniquely resolve important differences in productivity and fracture geometry. Diagnostics such as distributed acoustic sensing, microseismic, and sealed wellbore pressure monitoring capture total hydraulic fracture extent but do not characterize the producing behavior. Thus, it is very valuable to utilize diagnostics that directly assess the producing length and height of fractures. Vertical flow allocation is particularly important in formations with multiple productive benches, such as in the Midland Basin.

This work reveals the connection between completions, geomechanical inputs (such as minimum horizontal stress and toughness), and the geochemical production allocations as demonstrated by the vertical distribution of proppant. This work also identifies the roles that well spacing and drawdown play in time-lapse geochemical production allocations.

Introduction

With attention throughout the industry on delivering shareholder returns, unconventional oil and gas operators are intensely focused on maximizing capital efficiency. Operators have multiple design levers at their disposal carrying productivity and cost implications, including well spacing vertically and laterally, lateral length, stage spacing, cluster spacing, proppant loading, and fluid intensity.

Fig. 1 demonstrates a hypothetical design sensitivity with the wide range of possible outcomes for both value and resource recovery. Development optimization is challenging because of the complex array of design permutations and the variability of formation properties across a basin.

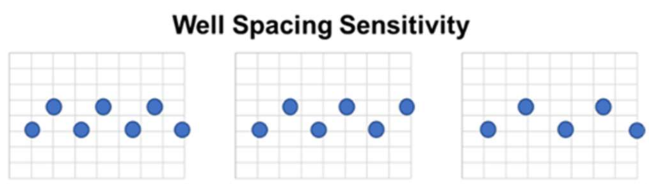

Completion Sensitivity

Stage	# Clusters	Fluid	Proppant	Cost
Short	Low	High	Highest	$$$$$
Short	Med	High	Highest	$$$$$
Med	Med	High	Highest	$$$$
Long	High	High	Highest	$$$$
Long	High	High	High	$$$$
Long	High	High	Med	$$$
Long	High	High	Low	$$$
Long	High	Med	Highest	$$$
Long	High	Med	High	$$$
Long	High	Med	Med	$$
Long	High	Med	Low	$$
Long	High	Low	Highest	$$
Long	High	Low	High	$$
Long	High	Low	Med	$
Long	High	Low	Low	$

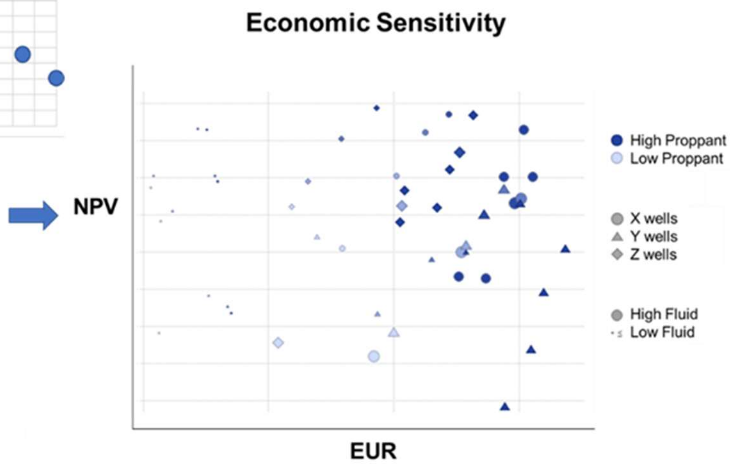

Fig. 1—A hypothetical well spacing, completion, and economic sensitivity.

Operators often turn to reservoir simulation to approach these challenges in a robust and cost-efficient manner. However, the utility of simulation models in unconventional assets can be limited by non-uniqueness in the history matching calibration phase. Multiple combinations of permeability, fracture geometry and connectivity, and resource distribution can lead to equally viable matches to production data. Utilizing models that match only production data for optimization sensitivities may lead to vastly different design implications for future development (Fowler et al. 2019).

Field diagnostics are used to reduce non-uniqueness. With sufficient fracture and reservoir characterization, it is possible to build a conceptual model predicting subsurface flow, and then use quantitative numerical modeling to perform economic optimization. Field diagnostic tools fall into two categories: (a) diagnostics from before wells go on production, and (b) diagnostics during well production. Diagnostic tools prior to production mainly characterize hydraulic fracture propagation and geometry, and include microseismic, distributed acoustic sensing (DAS), sealed wellbore pressure monitoring (SWPM), and permeability estimates from core analysis and diagnostic fracture injection tests (DFITs). Diagnostic tools studied during the producing time period include interference testing, downhole pressure monitoring, chemical tracers, and geochemical production allocation.

This paper focuses on geochemical analysis of produced hydrocarbons. Geochemical analysis allows for flow allocations by layer to be determined quantitatively. This fills a key niche in the toolbox of field diagnostics. These flow allocations provide quantitative information about the producing hydraulic fracture height over time. Models constrained by geochemical production allocation provide a credible starting point to subsequently optimize well spacing and completion designs in unconventional assets.

Flow allocations are simple to understand and incorporate into common workflows. They are provided in tabular format, which can be easily compared with the outputs from a simulation model. In this paper, we use case studies in the Permian Basin to demonstrate how geochemical production allocation can be used as a spatial and temporal constraint for unconventional reservoir simulation models. A companion paper by Albrecht et al. (2022) discusses how conservative tracers are also used to provide constraints on the productive fracture area.

Theory and Methods

Geochemical production analysis is used to determine the spatial origin and relative amount of specific produced fluids within a commingled stream. This technique has been used to understand conventional commingled production from different vertical completions as well as the origin of oil seepage (McCaffrey et al. 1996; McCaffrey et al. 2011; McCaffrey et al. 2012; Xing et al. 2019; Koksalan et al. 2020). The discussion in this paper focuses on analysis of oil composition, but the underlying concepts are also applicable to water and gas.

Petroleum fluids consist of thousands of different organic molecules, which are related to source rock type, thermal maturity, and reservoir conditions over time. The unique amount of each organic molecule forms what is referred to as its "oil fingerprint". In unconventional source rocks, individual geological layers have their own unique fingerprint. In-reservoir fingerprints can be established from core samples, cuttings, or from produced oil type wells over a vertical section. These subsurface geochemical fingerprints form a baseline to allocate produced fluids to each layer of reservoir. Hydraulically fractured wells often produce from multiple layers, commingling production from different layers with specific fingerprints. Gas chromatography is used to determine the relative abundance and/or ratios of specific organic molecules in the produced oil samples, which is then compared with the composition of the layer-specific fingerprints. Linear algebra is used to estimate the fraction of production contribution from the baseline oils. Specific methods are outlined in work by Liu et al. (2020), McCaffrey and Baskin (2016), and Jweda et al. (2017).

Fig. 2 depicts how hypothetical samples forming a baseline can be compared with produced oil from hypothetical Well A.

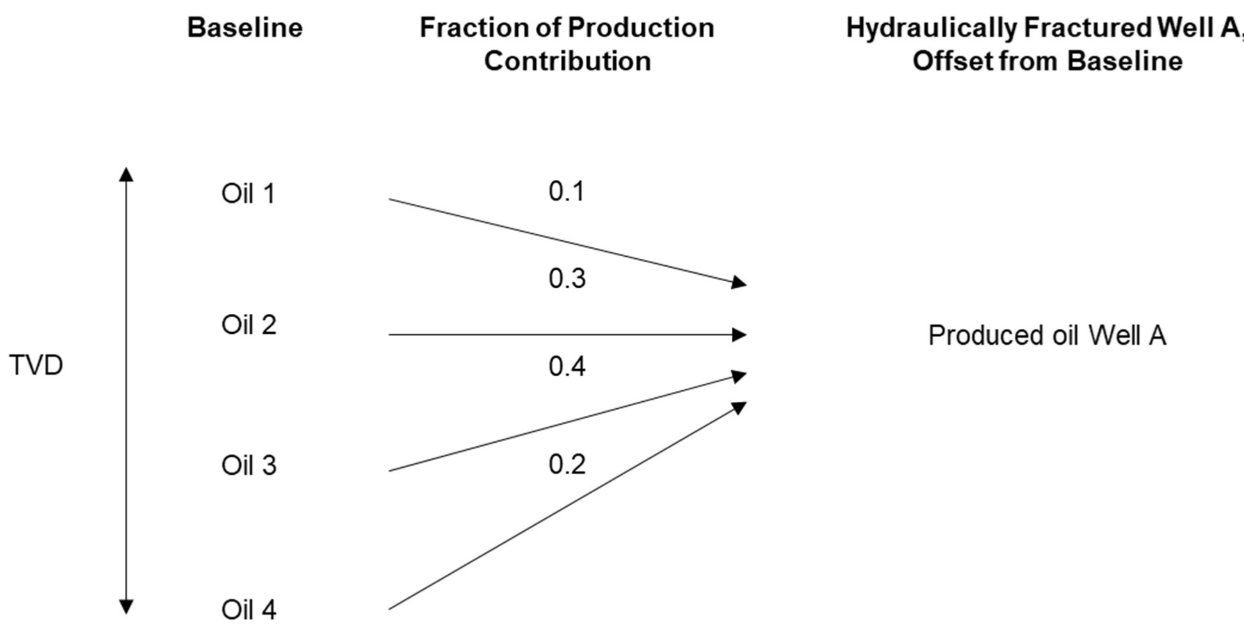

Fig. 2—Hypothetical baseline consisting of four unique oils used to allocate production from Well A.

Fig. 2 contains four unique fingerprints of analyzed oils from core, cuttings, or produced oil end-members. A produced oil sample from hydraulically fractured Well A is analyzed to back allocate its production contribution from unique oils 1, 2, 3, and 4. This allows for an understanding of the vertical drainage of Well A at any point during its producing life, shedding insight into the hydraulic fracture access and production from that wellbore.

The case studies include geochemical production allocations determined using the method outlined by Liu et al. (2020). Cuttings and/or core samples from three vertical wells were sampled and analyzed to form baselines located within the three regions specified in **Fig. 3**.

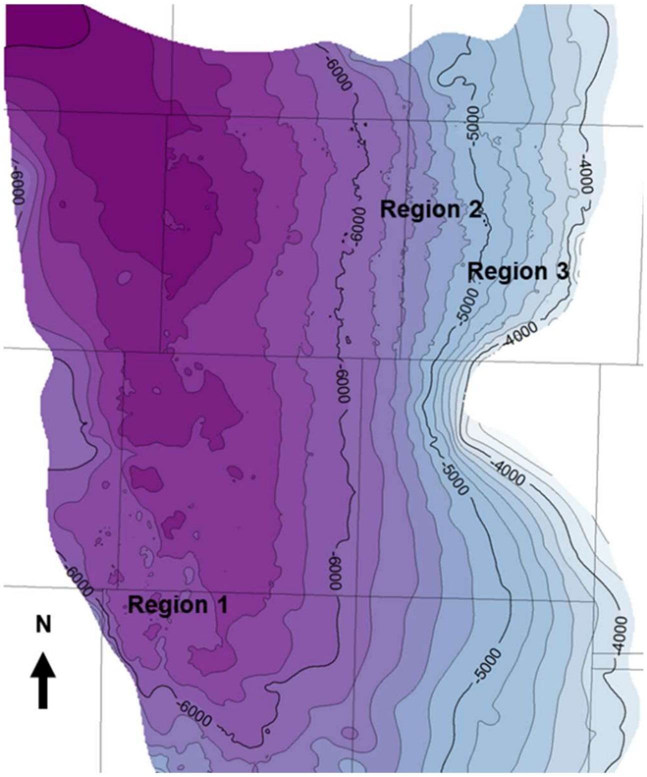

Fig. 3—Upper Wolfcamp structure map, Midland Basin.

The vertical resolution of the cuttings and/or core samples is on the order of 10 to 50 feet. Lateral variations in geochemical fingerprints by zone exist, therefore all horizontal wells evaluated in the case studies were located as close as practicable to the vertical well baselines. Some producing wells shared in the case studies had only one oil sample analyzed, others have one to three samples analyzed over the course of two years. An example of the geochemical production allocation diagnostics is shown in **Fig. 4**.

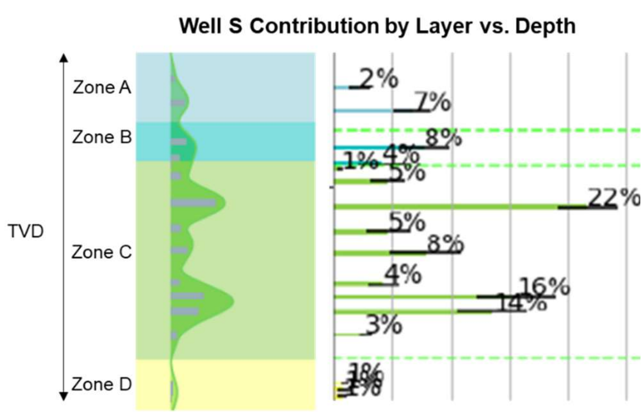

Fig. 4—Example of geochemical production allocation vs. true vertical depth.

Fig. 4 includes the geochemical production allocations from a hydraulically fractured well offsetting a vertical baseline. This information is for an oil sample taken at a given time from horizontal producer Well S, communicated as contribution by layer on the right side of the plot by the green bars vs. true vertical depth of the baseline well. The magnitude of the error for each layer contribution is indicated by the black horizontal lines. Individual layers may be part of a stratigraphic zone, indicated by the different colored shadings on the left side of Fig. 4. These results provided additional history matching constraints for the simulation models.

In the Midland Basin pictured in Fig. 3, operators develop the Wolfcamp and Spraberry formations through the drilling of horizontal wellbores with limited-entry completion designs to create hydraulic fractures via the pumping of proppant-laden fluids through perforations. The completion is an important production driver, and subsurface geomechanical properties largely control the hydraulic fracture geometry.

In this study, we used a three-dimensional simulator that couples hydraulic fracturing, geomechanics, and reservoir simulation (McClure et al. 2022). The simulator has capabilities that allow the user to generate flow allocations by layer over time that can be compared with geochemical allocation results.

For the simulations shown, a static model was developed containing subsurface petrophysical and geomechanical properties calculated from log measurements, core analysis, and DFIT measurements.

Additionally, bubble point with respect to depth was implemented in the simulation models. Approximate trends of formation volume factor, solution gas-oil ratio, viscosity, etc. were established from pressure-volume-temperature reports from produced oils drilled in unique landing zones across all regions discussed in the case studies.

The simulation models incorporated actual well configurations, including wellbore surveys and depths, perforation clusters, completion fluids, proppant volumes, and pump schedules. History matches were performed by specifying flowing bottom hole pressure, estimated from downhole and/or surface gauges with appropriate hydrostatic and friction loss correlations applied. In order to reduce model run-times without compromising accuracy, one full completion stage per well was modeled and total production rates were scaled proportionally. This approach assumes that individual completion stages contribute equally over time along the length of the lateral, which is a reasonable simplification for relative design comparisons.

The simulator provides two different methods for generating flow allocations for comparison with geochemical results. The first method tracks production into each fracture element by layer, and then allocates that production to the closest producing wellbore. The second method, which was not used in this paper, uses oil soluble tracers (see the section on future work).

Geochemical allocations are typically communicated visually as shown in **Fig. 5**. This plot shows fraction of geochemical production allocation by layer vs. TVD (also called ‘contribution vs. depth’). The light blue points represent contribution data generated by the simulation model, and the dark blue circles represent actual geochemical allocation data.

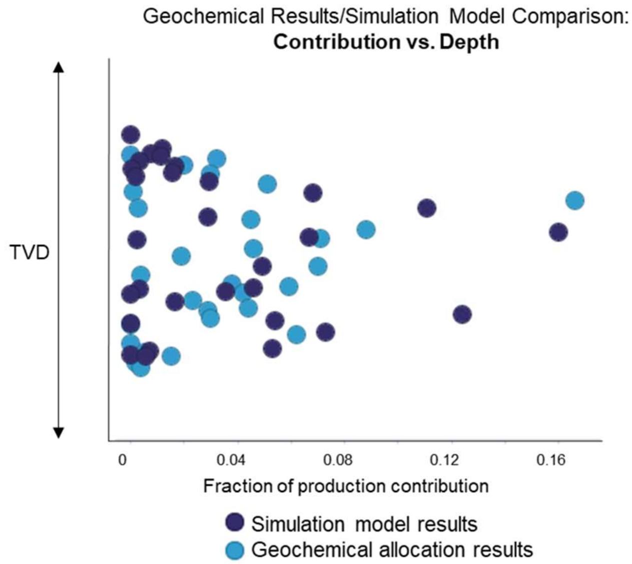

Fig. 5—A comparison between modeled and actual geochemical production allocation vs. depth.

There are challenges with comparing geochemical results with modeled results. The layers defined in the simulation model do not correspond precisely with the geochemical control points based on the core/cuttings samples, which may give the appearance of mismatches. The simulation models discussed in the case studies in this paper have vertically upscaled bins ranging in thickness from 5 to 200 feet, which is typically a much coarser upscale than what is offered through actual core or cuttings sampling.

The second challenge is that the plot appears erratic in terms of contributions. For those analyzing this data, this gives the first impression of variability in permeability. However, this is largely an artifact of upscale bin size and sampling interval.

To resolve these challenges, it is useful to compare the cumulative contributions vs. depth as shown in the right side of **Fig. 6**.

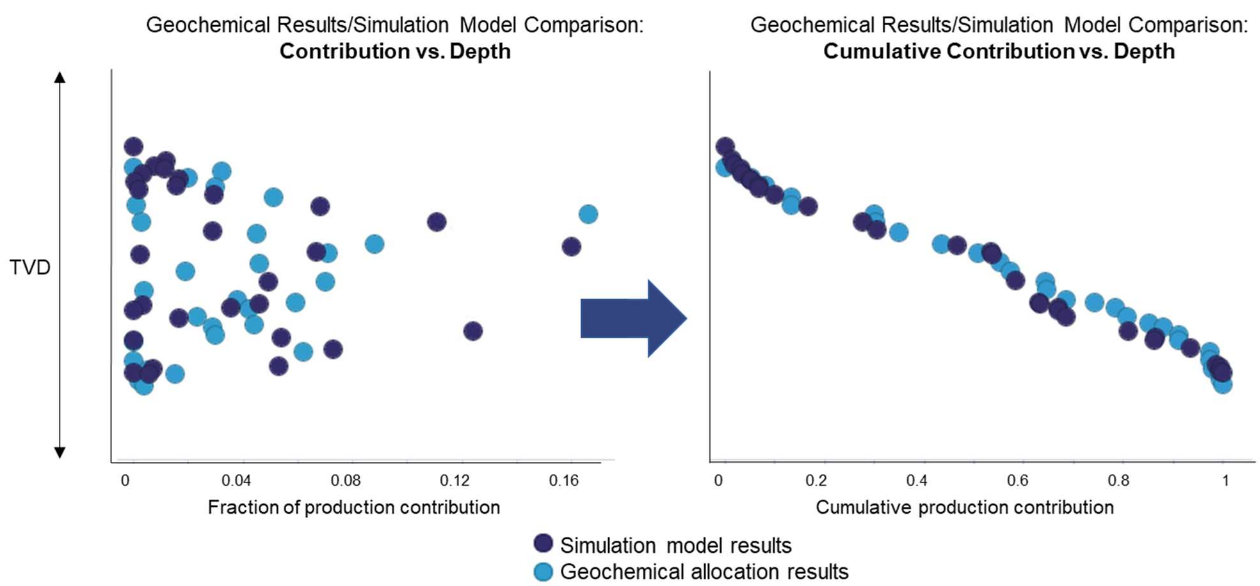

Fig. 6—Introduction of cumulative production contribution derived from contribution vs. depth.

The plot on the right side of Fig. 6 is produced by summing the individual contributions by layer over the total depth of contribution. This makes it much easier to visually compare the simulation results with the geochemical production allocation results, despite the differences in upscale thickness and baseline sampling. Both geochemical allocations and modeled results align, and results appear continuous and not erratic. This behavior is indicative of small contributions from low permeability rock at each depth over large heights.

Results

Case Study I

This case study discusses wells within Region 1 (Fig. 3). **Fig. 7** contains five log tracks from left to right including gamma ray (GR), facies, minimum horizontal stress, vertical well geochemical sample coverage, and modeled and actual cumulative contribution vs. depth. Horizontal wells were landed within two stratigraphic zones relative to this pilot well and denoted on the stress track.

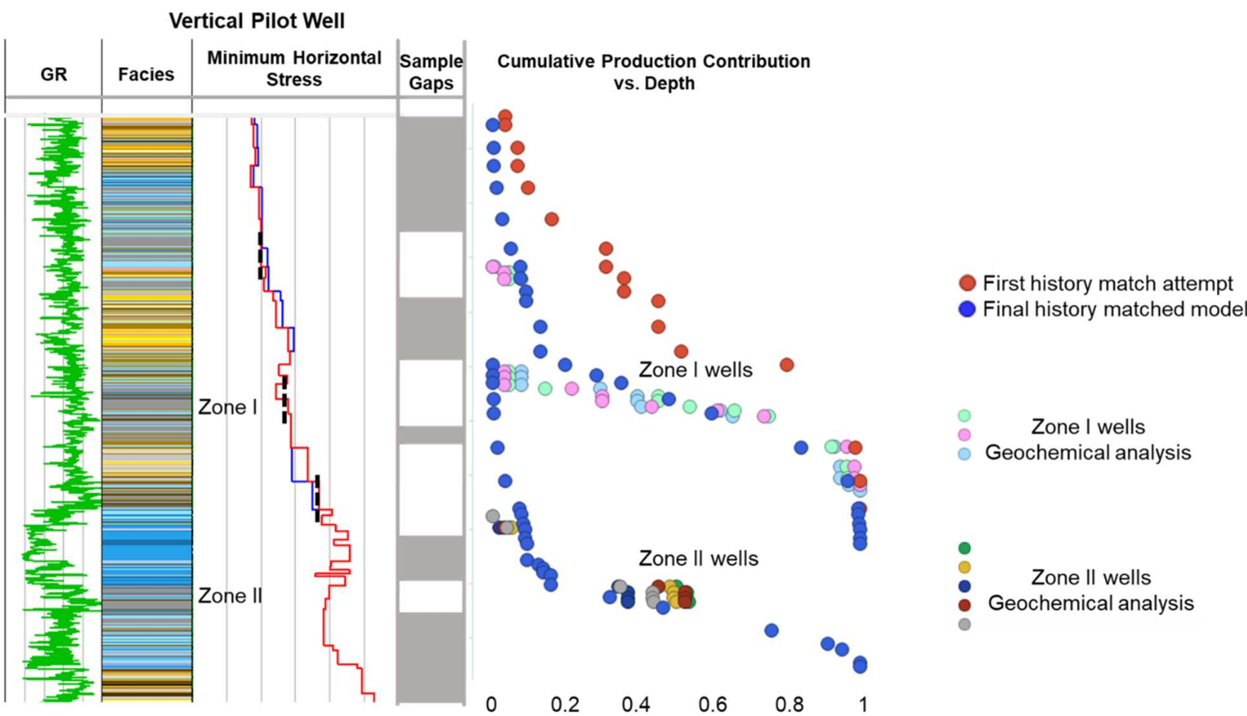

Fig. 7—Comparison between log properties and simulation models producing geochemical allocations in Case Study I.

The vertical control well for geochemical production allocation used limited sampling via sidewall cores. The fourth track in Fig. 7 shows vertical coverage of depths available for geochemical analysis, with gray indicating the location of these gaps in sampling. This limited vertical coverage likely introduced uncertainty in the resulting geochemical production allocation. Additionally, produced oil samples were unavailable for the modeled wells, so offset wells in the same stratigraphic landing zones and completion designs at similar sampling intervals close to the vertical control well were used for history matching production allocation. The allocations from several offset wells in each stratigraphic zone are shown in the multi-colored circles, with each unique color representing the allocations from unique offset wells. The simulation model results are shown in red and blue circles.

The first attempt to model wells in Zone II resulted in good matches with offset well geochemical production allocation results. However, sample gaps deeper within Zone II created an unknown contribution depth extent for approximately half of the production of Zone II wells.

The Zone I wells required additional calibration to match geochemical production allocation results. The minimum horizontal stress profile from the first attempt at history matching is shown in red (Fig. 7), along with offset well DFIT measurements of minimum horizontal stress, shown in black dashed vertical lines at similar stratigraphic depths. Also indicated in red in the track of cumulative production contribution is the preliminary outputs of production allocation from the simulation models. Note that shallow contribution was significantly overpredicted relative to contributions suggested via geochemical production allocation. This overprediction in modeled shallow contribution is controlled by what stratigraphic zones hydraulic fractures access. Vertical access in the model is controlled by the completion (known) and model inputs of minimum horizontal stress.

While there are numerous methods available to estimate a continuous minimum horizontal stress, all have uncertainty and require calibration. Direct measurements of minimum horizontal stress are preferred and are often collected in the form of closure measurements from DFITs pumped in the toe stages of horizontal wells. However, DFITs are not always available at every stratigraphic depth, and so estimates are made continuously at every depth usually driven from logs. This example clearly shows the value of the geochemical data used within this workflow to help reduce uncertainty in the calculated stress where it was not directly measured.

The minimum horizontal stress profile in blue shows slight modifications made to the red profile (Fig. 7). These slight changes resulted in the modeled cumulative contribution vs. depth in blue drastically shifting toward reduced contribution from shallower intervals as well as increased contribution from deeper intervals. The changes to the stress profile were mostly made in intervals where DFIT data from offset horizontal wells was not available and there was uncertainty in the log derived stress. While these changes mainly affected the small tails representing <10% of contribution at the sampled time, it is thought that these small contributions may impact vertical well spacing choices.

Fig. 8 shows the simulation model in profile view along a single completion stage of the modeled horizontal wellbores. The colored planes contain the pressure within the hydraulic fractures. The left image of Fig. 8 shows the hydraulic fracture growth using the first minimum horizontal stress profile in red from Fig. 7. The right image shows the fractures resulting from utilizing the blue minimum horizontal stress profile. While the final history match maintained hydraulic fracture growth into shallower intervals, the overall magnitude of hydraulic fracture growth is less than the first model iteration.

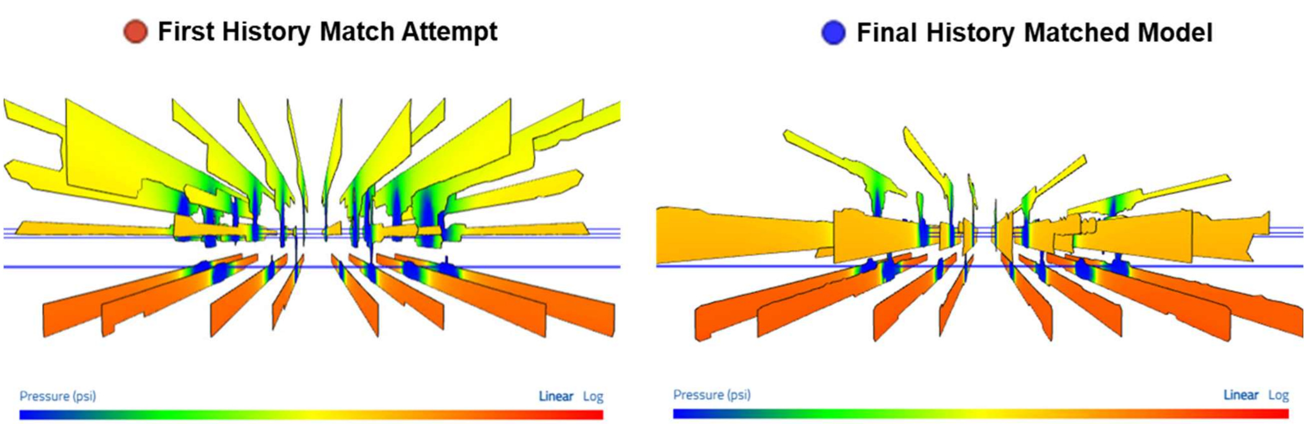

Fig. 8—Comparison of modeled fracture geometries using two different stress profiles in Case Study I.

Given the agreement between geochemical production allocation and modeled results in Fig. 7, we interrogated the calibrated model's future production behavior. Time-lapse allocations were unavailable for the Zone I wells with geochemical production allocations shown in Fig. 7, but offset Well J had geochemical allocations available at one and two years into production. Well J used a different completion and offset well spacing, thus is not a perfect analog. The time-lapse data of both geochemical and modeled results are shown in **Fig. 9**.

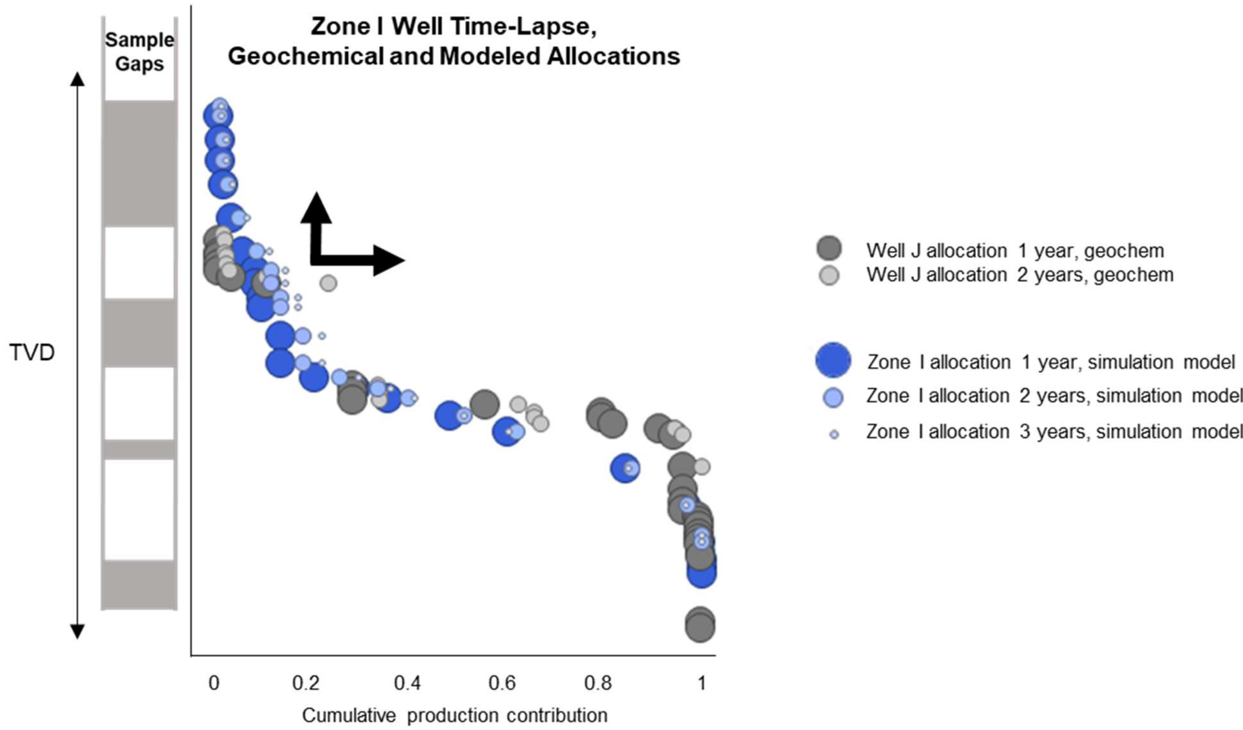

Fig. 9—Time-lapse comparison between Well J geochemical production allocation results and Zone I modeled wells.

The time-lapse samples in Fig. 9 are sized and colored by production time, with the earlier times represented by larger, darker circles and later times by smaller, lighter circles. Geochemical allocations from Well J are colored in shades of gray, and modeled results are colored in shades of blue. Note that both Well J and the Zone I modeled well are not bounded by any shallower wells, only wells in deeper formations. Both actual and modeled data suggests increased contributions from shallower zones with longer producing time, as shown by the black arrows in Fig. 9.

Case Study II

Case Study II focused on history matching with geochemical allocation results to constrain modeled results in Region 3 (Fig. 3).

Fig. 10 contains log properties for vertical Well M and Well N within Region 3. A simulation model was created of offset horizontal producer Well P using geochemical production allocation data from a sample taken in its second year of production and rate data. The log tracks in Fig. 10 from left to right include GR, facies, minimum horizontal stress, and cumulative production contribution from geochemical allocations and simulation models for Well P two years into production in blue and orange respectively.

Well M pictured on the left side of Fig. 10 was originally chosen for the simulation model vertical control well as it had core and cuttings available for baseline geochemical analysis, data required for the geomechanical model, and was near Well P. The first simulation model results showed a large mismatch with geochemical allocation results of Well P. Modeled production contribution in orange indicated shallower contributions than what was suggested by geochemical results in blue. High stresses in the deeper portion of Well M shown in the red box in Fig. 10 prevented downward growth of hydraulic fractures in Well P, which resulted in limited production from these deeper intervals within the simulation model.

Upon further investigation, it was noted that other nearby vertical wells in Region 3 with geomechanical properties, such as vertical Well N, exhibited different log character in the deeper portion of the well where the model results diverged from geochemical allocation results. Well N had different facies distribution and lower stress in the deeper zones as compared to Well M, seen in Fig. 10. Therefore, minimum horizontal stress was decreased, and facies and corresponding oil saturations were adjusted in the deeper stratigraphy in the Well P simulation model to align closer with the Well N observed properties. This resulted in deeper access of Well P hydraulic fractures in the model. Subsequently the Well P history match of geochemical production allocation improved, as is viewed in the right side of Fig. 10 vs. Well N log properties.

This demonstrates the importance of understanding the regional variability of subsurface geological, petrophysical, and geomechanical properties. Ideally, a 3D model of subsurface properties should be used, such that actual properties at the location of the horizontal well are used in the simulation.

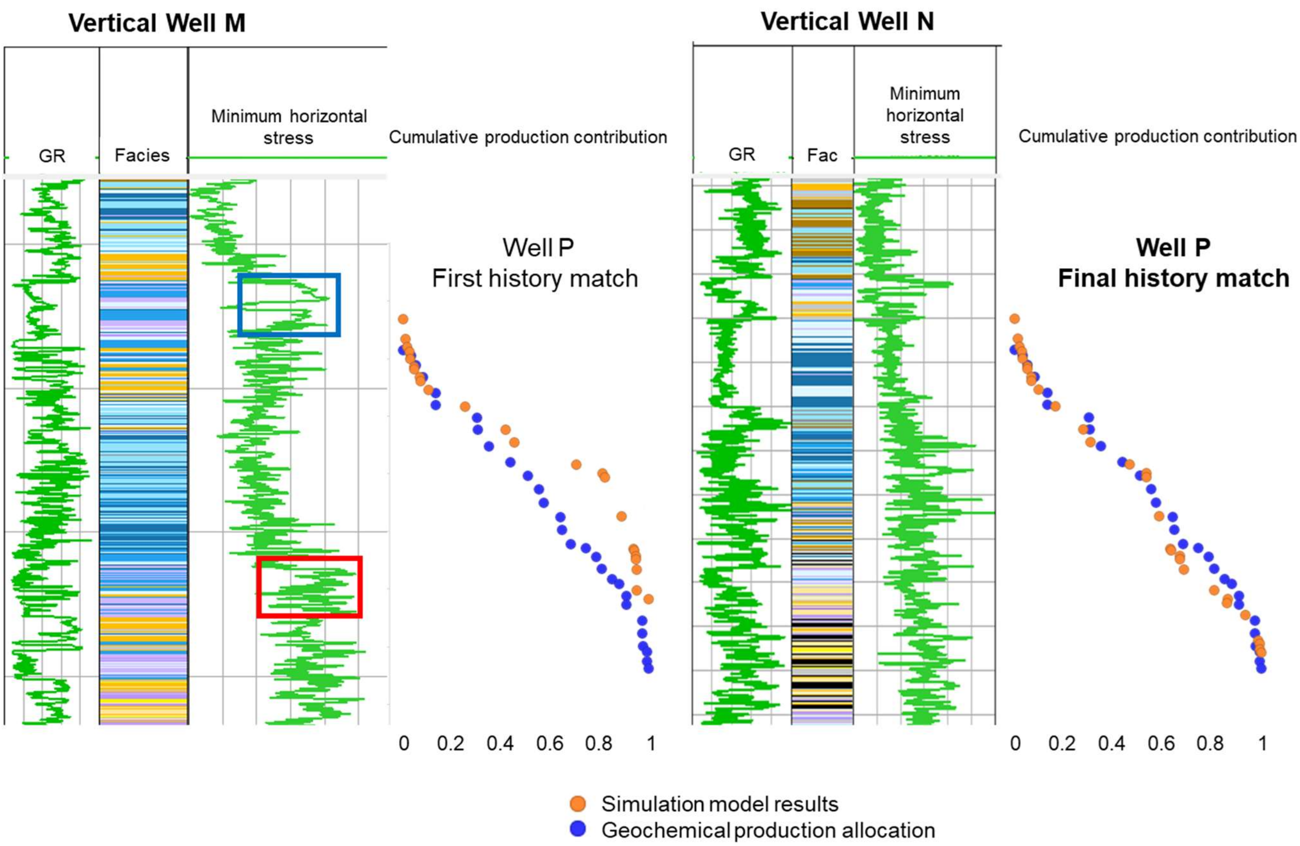

Fig. 10—Comparison of modeled production allocations relative to two different stress profiles in Region 3, Case Study II.

The lack of asymptote in the shallowest end of the cumulative production contribution curve that is aligned with high minimum horizontal stress boxed in blue in Fig. 10 suggests that vertical barriers to hydraulic fracture growth exist. This is also observed within the simulation model of Well P. Shown in **Fig. 11** are the hydraulic fractures of Well P in gray versus a cross section through the wellbore (not pictured) of simulation matrix cells showing minimum horizontal stress. Note the high stress intervals above and below the hydraulic fractures preventing vertical growth.

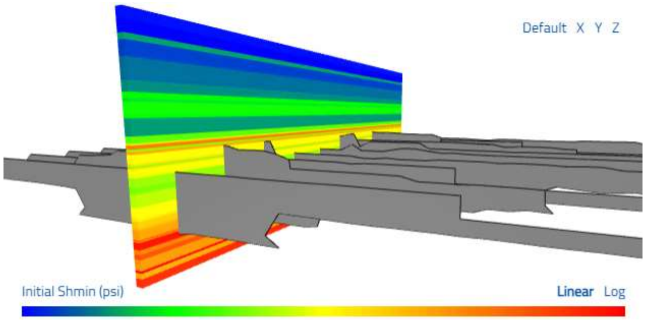

Fig. 11—Modeled hydraulic fractures from Well P versus matrix properties of minimum horizontal stress, Region 3, Case Study II. Note the high stress regions preventing hydraulic fracture growth.

Case Study III

The third case study shares a history match of geochemical production allocation data seven months from the start of production of a hydraulically fractured horizontal well in Region 2 (Fig. 3). Shown in **Fig. 12** are logs of GR, facies, and minimum horizontal stress of vertical Well Q. DFIT measurements of stress from nearby offset horizontal wells are stratigraphically extrapolated to Well Q and are plotted in vertical black lines vs. the original upscaled minimum horizontal stress profile colored in red.

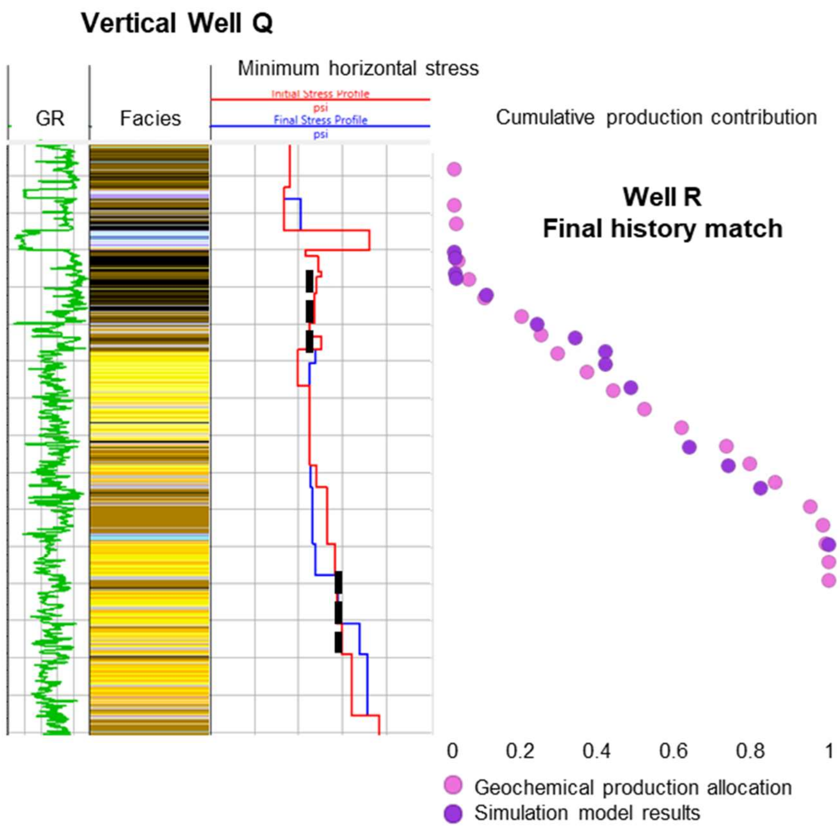

Fig. 12—History matched model of Well Q production allocations versus geochemical production allocation results, Region 2, Case Study III.

A simulation model was built of horizontal producer Well R offset from vertical Well Q. The upscaled minimum horizontal stress used in the final history match model is plotted in blue. Like Case Study I, only slight changes to minimum horizontal stress in red were required to arrive at the final history match shown in the cumulative production contribution track in purple. Again, these changes occurred in intervals without offset stress measurements. This highlights both the value of stress measurements as well as geochemical data to help constrain the simulation results. There is good agreement between the final history match of cumulative production contribution and the interpretation from geochemical production allocation results.

Case Study IV

The final case study focuses on wells within a multi-well parent/child development with time-lapse geochemical production allocation results. This development took place in Region 2 (Fig. 3) and is shown in **Fig. 13**.

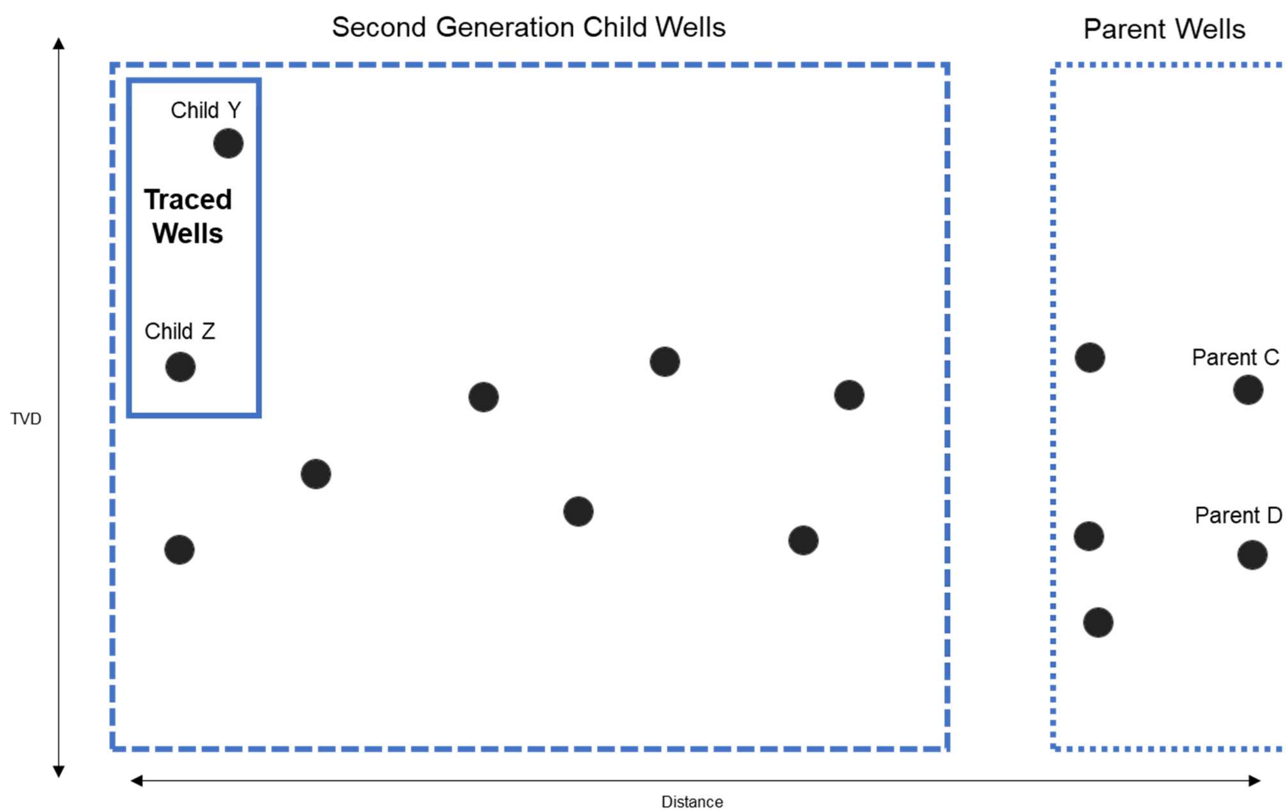

Fig. 13—Gun barrel view of parent/child development with tracer data and geochemical production allocation results, Region 2, Case Study IV.

Child Y, Child Z, and seven additional child wells were developed offset from five parent wells. A model of this development scenario was built and history matched using quantitative tracer analysis described in the companion paper by Albrecht et al. (2022). Tracers were injected into Child Y and Child Z during completion. Key findings from this history match included tracer transport from Child Y and Child Z to Parent C and Parent D and offset child wells in between, as well as tracer transport between Child Y and Child Z.

Time-lapse geochemical production allocation results of Child Y and Child Z were acquired after initial modeling. Produced oil samples from Child Y and Child Z were collected at 3 days, six months and two years into production. Results comparing the time-lapse contributions from geochemical results are shared in **Fig. 14**.

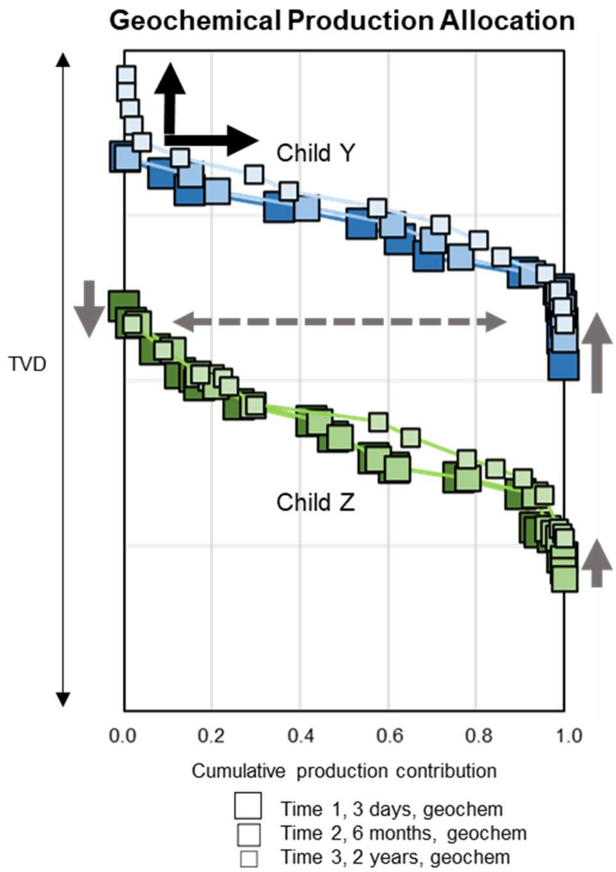

Fig. 14—Time-lapse geochemical production allocations from Child Y and Z, Region 2, Case Study IV.

In Fig. 14 the squares are sized and colored by sample, with the largest, darkest sample representing early time data and the smallest, lightest squares representing the two-year samples.

Child Y was only bounded by Child Z beneath, no wells were located shallower. Child Y production allocations showed an overall increase in its shallower vertical extent and production contribution over time, denoted by the black arrows. While overall production is lower two years into production, the extent of the contribution has shifted with contribution from shallower zones having increased. These two-year allocations with tails not seen in earlier samples suggest Child Y is beginning to deplete shallower and further away from its target zone due to the lack of wells shallower than Child Y. This is in contrast with the lack of observed tails in two-year allocations of Well P from Case Study II, where stress barriers to vertical hydraulic fracture growth were inferred.

In contrast with the bounding of Child Y, Child Z was vertically bounded both by Child Y shallower and an additional deeper well. The vertical extent of actual time-lapse geochemical production allocations for Child Z contracted over the three samples, denoted by the gray vertical arrows next to its cumulative production curve. The vertical extent of Child Y contribution decreased in its deeper access, denoted by the gray arrow next to its cumulative production curve. The drainage extent of both Child Y and Child Z appeared to retreat from each other over time to a similar depth, as noted by the gray dashed line and gray arrows (Fig.14).

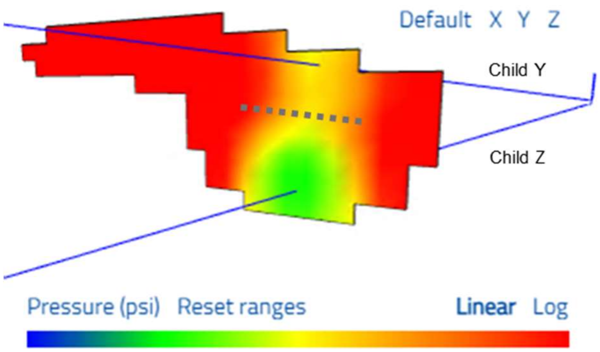

Fig. 15—View of pressure within a modeled hydraulic fracture from Child Z showing hydraulic connection with Child Y.

The changing flow allocations over time can be better understood by examining the detailed simulation outputs. **Fig. 15** shows the pressure distribution in a particular hydraulic fracture after two years of production. Both Child Z and Child Y are hydraulically connected to the fracture and drawing down pressure. The dotted gray line in Fig. 15 shows the approximate drainage divide where fluid flows upward to Child Y or downward to Child Z. The time-lapse geochemical production allocations of Child Y and Child Z demonstrate this inter-well communication through the reduction in the tails seen in Fig. 14 at the depth indicated by the dashed gray line. The observations of inter-well communication are also validated by tracer transport, interference testing and estimated ultimate recovery of both child wells as compared to standalone counterparts.

Results comparing the time-lapse contributions from geochemical results and the simulation model are shown in **Fig. 16**.

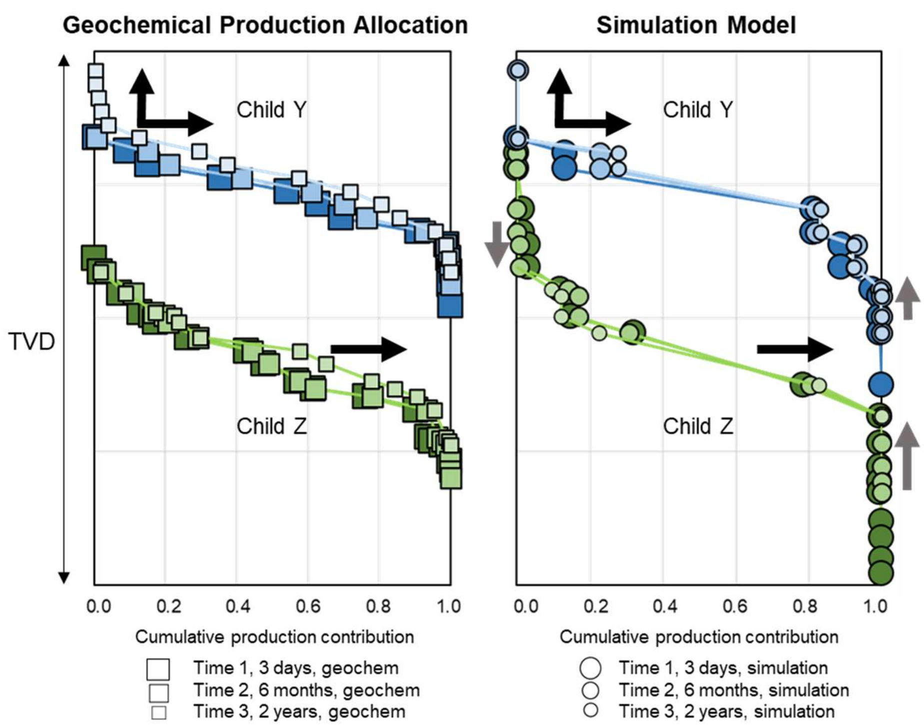

Fig. 16—Comparison between time-lapse geochemical production allocations and modeled results for Child Y and Z, Region 2, Case Study IV.

Squares represent geochemical production allocations and circles represent results from the history matched simulation model. Both are sized and colored by time on production, with the larger, darker icons representing early time and the smaller, lighter shapes representing later time data. Fewer overall circles are present as a result of the coarse model upscaling.

Overall, there is good agreement between the time-lapse cumulative production contribution of the geochemical production allocation and simulation model for both Child Y and Child Z. Just as the actual geochemical production allocations revealed, the modeled drainage extent of both Child Y and Child Z appeared to retreat from each other over time as indicated by the gray arrows. Child Y and Child Z modeled results exhibit increased shallow contribution with time denoted by the black arrows in the non-overlapping regions of their profiles.

As previously mentioned, Child Y is bounded by wells in deeper zones but unbounded in shallower intervals. By two years of production, Child Y geochemical and modeled results both show shallowing in the vertical drainage extent over time, as denoted by the black vertical arrows. This is like the production behavior of time-lapse Well J and the Zone I model in Case Study I (Fig. 9), which were also bounded only by deeper wells. In contrast, Child Z (also located in Zone I) was bounded both by shallower and deeper wells. The Child Z vertical production extent retreated in line with its bounding from both shallower and deeper wells, opposite of what was observed in the shallow contributions over time from Zone I wells in Case Study I (Fig. 9). This suggests geochemical allocation results are influenced by development well spacing.

The model settings and actual boundary conditions that produced the geochemical production allocation shared in this case study involved producing all wells according to their flowing bottom hole pressure. In this example, all wells began production at the same time using similar artificial lift allowing for similar well pressure drawdown. This means that the geochemical production allocation results observed in this case study were a function of the operating conditions of each well and its neighbors. Had Child Y been shut-in, or non-existent, geochemical production allocation for Child Z should look different over time.

The time-lapse geochemical and model results from three wells in Case Studies I and IV showed increased shallow contribution and extent from unbounded wells vs. bounded wells. This suggests that the well spacing and bounding of wells impacts the observed geochemical production allocation, and that the shallow extent and/or contribution of well drainage over time may increase in the absence of vertical bounding by other wells or barriers to hydraulic fracture growth. This observation is also corroborated by known differences in estimated ultimate recovery of wells with varied spacing. This observation means that geochemical production allocation quantifies inter-well communication, which is what operators try to understand so they can optimize well spacing in future developments. A model capturing this behavior is well calibrated for use in well spacing and completion design sensitivities.

Discussion

The case studies shown in this paper leveraged extensive prior history matching that constrained fracture toughness inputs with quantitative tracer data (Albrecht et al. 2022). Only slight model adjustments were required to match the geochemical production allocation data once it was available. The matches between modeled and actual allocations are corroborated by tracer data and DAS. These robust history-matched models have higher confidence when applied in well spacing and completion sensitivities.

The first three case studies demonstrated that slight modifications to minimum horizontal stress profiles resulted in improved history matches with respect to comparisons of modeled vs. actual geochemical production allocation over time. These adjustments were on the order of 100-200 psi, representing a low variance from original estimates. Modifications were typically made in zones where direct measurements of stress via DFITs were not available.

The adjustments to modeled minimum horizontal stress resulted in reduction of model vs. geochemical allocation mismatches from approximately 40% to less than 10% around any given layer. Since (a) simulation model upscaling was coarser than geochemical baseline sampling, (b) changes to other input parameters were not studied as an alternative to stress modifications, (c) numerous other samples not shared within this paper were also compared and (d) associated error of geochemical allocations in any given layer is on the order of 3%, these remaining discrepancies between models and geochemical production allocation results were deemed acceptable for future sensitivity models.

These case studies demonstrate the value of utilizing geochemical data as a calibration tool. With a more accurate history match, there is more confidence in accurate forward modeling of different well spacing and completion design scenarios that are important to operator pad development.

The geochemical production allocation data from Case Studies I, II, and III is shown **Fig. 17**.

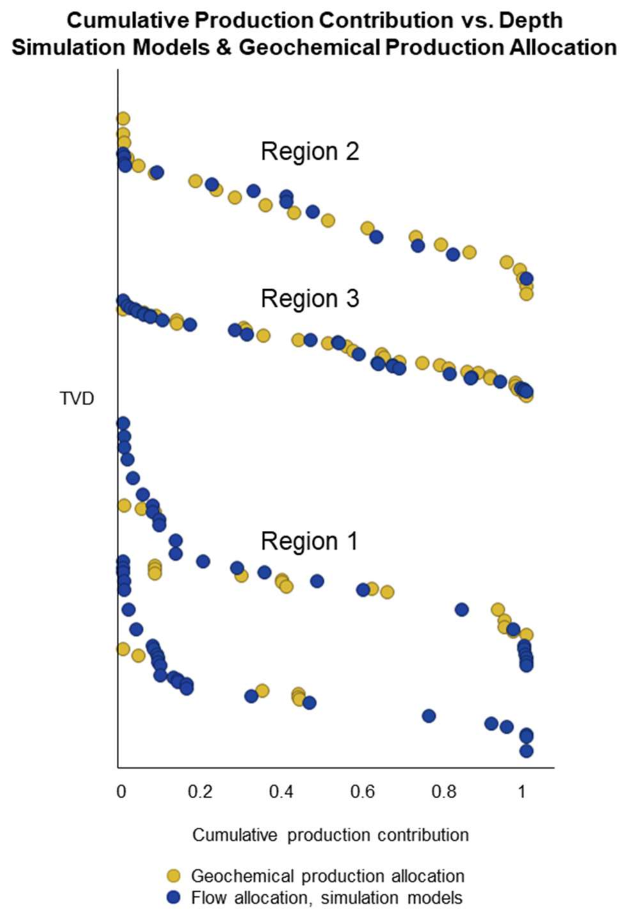

Fig. 17—Comparison between geochemical analysis and modeled results for wells in four landing zones in Case Studies I-III.

The analysis in Fig. 17 spans three regions and four distinct landing zones. Actual (gold) and modeled results (blue) match. Both exhibit relatively uniform production behavior across the reservoir interval as demonstrated by the straight lines of contribution versus depth. Relative permeability to oil in models in all landing zones and regions is also similar, and all models use fluid properties that vary with respect to depth. Regional trends in vertical variability in model inputs such as mobile hydrocarbons, pore pressure, and geomechanical inputs are consistently honored in all models across the Midland Basin case study wells. This suggests similar production mechanisms across regions and landing zones within the areas modeled in the Midland Basin (Fig. 3). Viewing production allocation in terms of cumulative contribution instead of relative contribution enabled these observations.

History matches in all case studies were achieved with planar fracture geometries, which is consistent with recent published core-through and fiber optic diagnostics in the Midland Basin and other shale plays (Gale et al. 2018; Shahri et al. 2021). Figs. 8, 11, and 15 all depict these planar hydraulic fractures.

This work demonstrated that modeling limited entry completions with respect to geomechanical inputs including minimum horizontal stress resulted in flow allocations that closely matched geochemical production allocation results. In contrast, others have used discreet fracture network (DFN) models, natural fractures, and tuned assumed hydraulic fracture properties to match geochemical allocations (Rasdi et al. 2012).

While natural fractures have been observed in core-through studies (Gale et al. 2019), the simulation models shared in these case studies did not contain natural fractures and were not required to match production rates or geochemical production allocation. All wells modeled have similar behavior in the relatively straight lines of cumulative production contributions, suggesting oil relative permeability, fracture conductivity, and the overall model transmissibility is appropriate. All models also use similar proppant trapping settings.

Proppant Distribution

Given the agreement between geochemical production allocation and modeled results, we can interrogate the calibrated models to investigate key performance drivers. For each of the wells in Fig. 17 the modeled proppant distribution was normalized versus the total mass of proppant injected in each well. **Fig. 18** shows the vertical distribution of proppant in hydraulic fractures from wells in the three regions.

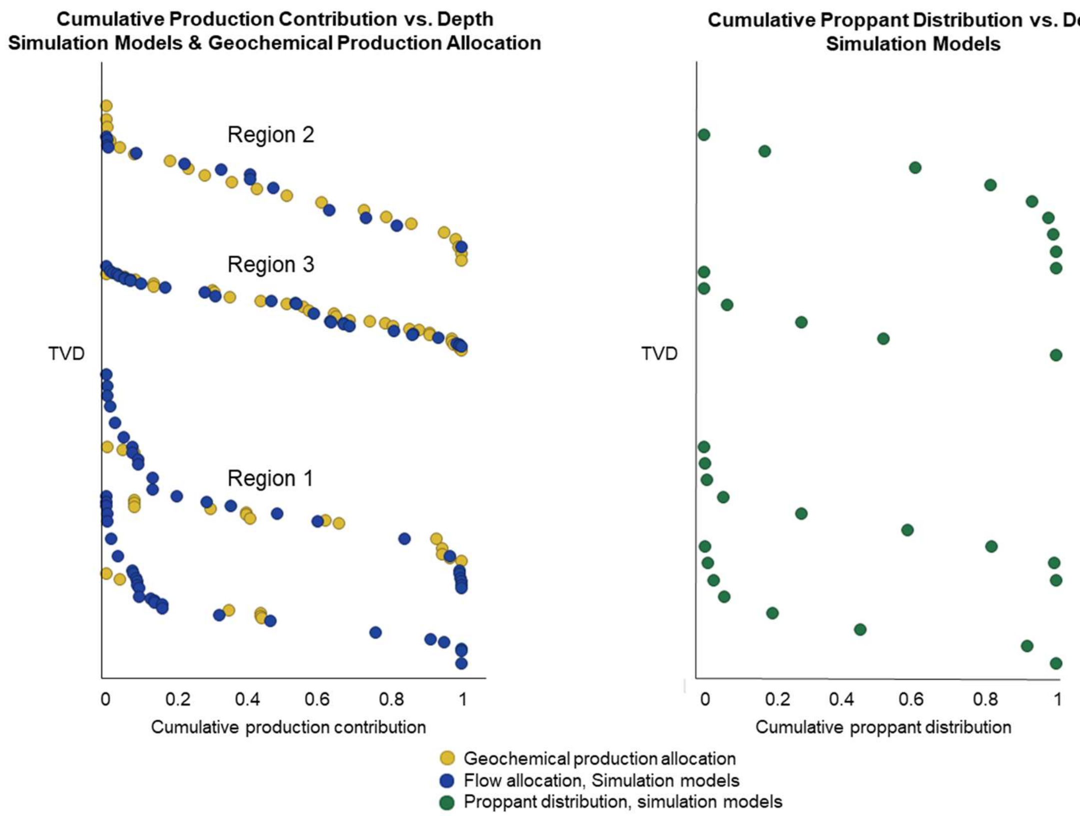

Fig. 18—Comparison between geochemical analysis and flow allocations from simulation models and the location of proppant within the models for wells in four landing zones from Case Studies I-III.

Comparisons between the plots in Fig. 18 suggest that a close relationship exists between the location of proppant and the resulting production contribution. It should be noted most of these wells are in zones with vertically continuous oil saturations. If there had been greater variability in oil saturation, the relationship between proppant placement and production may have been more variable, as observed in the well located in Region 2 and to a lesser degree Region 3 (Fig. 18). The geochemical results suggests that proppant is placed over hundreds of feet vertically.

For all wells in Fig. 18, the proppant distribution did not follow a consistent pattern with respect to landing depth. Sometimes the proppant was located 60% below the landing zone, sometimes 85% above. This depended on the complicated nature of the subsurface including earth stresses, toughness, layering, and interface properties, as well as fracture-to-fracture stress shadowing.

Uncertainties

Simulation models sometimes suggest vertical production contribution in excess of the heights and magnitudes indicated by the presence of small tails (<5% contribution) on these modeled curves. This was deemed plausible given the sample gaps in geochemical vertical well control in Region 1. This was also observed within the Case Study IV wells in Region 2. Similarly, vertical hydraulic fracture growth to shallower intervals was extensive within both Case Study I and IV models. Only very small amounts or no proppant were found in these shallower depths within the models. This raises questions about the extent of production contribution from unpropped hydraulic fractures. Additional produced oil samples over a longer producing time will be helpful to understand their contribution, as well as additional investigation into the magnitude of uncertainty in the geochemical allocation process itself in relation to these small tails. These seemingly small tails may have economic implications for vertical and lateral well placement which should be considered.

Actual data produced by geochemical production allocation is not necessarily transferrable across landing zone alone. Case Studies I, II and III illustrated geochemical production allocation results reflect completion design choices through the strong correlation between cumulative production contribution with the cumulative distribution of proppant. Case Study IV illustrated geochemical production allocation results over time reflect a given well spacing and pressure drawdown. Therefore, changing the completion design, well spacing, or operating conditions will result in unique allocations over time. Results are not necessarily applicable if a drastically smaller or larger completion design was pumped, different vertical or lateral spacing is implemented, or different operating conditions are applied.

Future Work

As discussed above, the modeled flow allocations in this paper used a heuristic that assigned production from a fracture element to the closest producing well. However, after this work was performed, a more realistic method for quantifying flow allocations was implemented into the simulator. The simulator permits the user to define oil or gas soluble tracers as part of a 'black oil' fluid model. A unique oil soluble tracer can be placed in each layer, as a part of the model initialization. The simulator rigorously solves mass balance on all tracer components in each timestep, providing a fully realistic flow allocation by layer, based on the actual solution to the flow equations. This capability will be used in future work.

All case studies shared within this paper included geochemical production allocation results from produced oil samples taken starting at 3 days to no more than two years into production. As wells within the Midland Basin are expected to be long lived, geochemical production allocation has relevance for samples taken at 5, 10, 15+ years of production beyond what is currently available. These additional time-lapse samples are critical to understanding and constraining models with unpropped versus propped hydraulic fractures. Applying this workflow to vintage Wolfberry vertical wells could shed light on longer term production behavior in areas with younger horizontal wells.

Conclusions

1. This paper demonstrates the utility of geochemical production allocations for constraining hydraulic fracture and reservoir simulation models. The allocations allow the hydraulic fracture geometry to be fine-tuned, resulting in better calibrated models for optimizing well placement and completion designs.
2. In the case studies, the simulation allocations were matched to the geochemical allocations using small adjustments to the minimum horizontal stress profiles at depths lacking direct measurements from DFITs. This highlights the importance of stress measurements as well as the use of geochemical production allocation results for calibration.
3. Viewing geochemical allocation results in terms of cumulative contribution rather than contribution by layer revealed relatively uniform production mechanisms across all regions and landing zones and available timestamps.
4. Simulation models were able to capture time-lapse geochemical production allocation behavior with respect to communicating wells and drawdown. Vertical bounding by other wells or barriers to hydraulic fracture growth likely affect both geochemical allocations and modeled results over time.
5. Geochemical allocation results correlate to the vertical distribution of proppant within the hydraulic fractures and petrophysical overlay of oil saturation.
6. The distribution of proppant showed no fixed relationship with respect to landing zone, and instead appeared to be largely controlled by the completion and its interaction with geomechanical properties.
7. Hydraulic fracture geometries resulting from matching geochemical production allocation results were independently corroborated with other diagnostic tools such as DAS and chemical tracers.

References

Albrecht, Magdalene, Borchardt, Shannon, Murphree, Chase, McClure, Mark, and Janz Rondon. “Using Quantitative Tracer Analysis to Calibrate Hydraulic Fracture and Reservoir Simulation Models: A Permian Basin Case Study.” Paper presented at the SPE/AAPG/SEG Unconventional Resources Technology Conference, Houston, Texas, USA, June 2022. doi: https://doi.org/10.15530/urtec-2022-3724108

Fowler, Garrett , McClure, Mark , and Craig Cipolla. "A Utica Case Study: The Impact of Permeability Estimates on History Matching, Fracture Length, and Well Spacing." Paper presented at the SPE Annual Technical Conference and Exhibition, Calgary, Alberta, Canada, September 2019. doi: https://doi.org/10.2118/195980-MS

Gale, Julia F. W., Elliott, Sara J., and Stephen E. Laubach. "Hydraulic Fractures in Core From Stimulated Reservoirs: Core Fracture Description of HFTS Slant Core, Midland Basin, West Texas." Paper presented at the SPE/AAPG/SEG Unconventional Resources Technology Conference, Houston, Texas, USA, July 2018. doi: https://doi.org/10.15530/URTEC-2018-2902624

Gale, Julia, Elliott, Sara, Li, John Z., and Stephen Laubach. "Natural Fracture Characterization in the Wolfcamp Formation at the Hydraulic Fracture Test Site (HFTS), Midland Basin, Texas." Paper presented at the SPE/AAPG/SEG Unconventional Resources Technology Conference, Denver, Colorado, USA, July 2019. doi: https://doi.org/10.15530/urtec-2019-644

Jweda, Jason, Michael, Eric, Jokanola, Olufemi A., Hofer, Robert, and Victoria A. Parisi. "Optimizing Field Development Strategy Using Time-Lapse Geochemistry and Production Allocation in Eagle Ford." Paper presented at the SPE/AAPG/SEG Unconventional Resources Technology Conference, Austin, Texas, USA, July 2017. doi: https://doi.org/10.15530/URTEC-2017-2671245

Koksalan, Tamer , Ahsan, Syed Asif, Azouq, Youcef , Alhouqani, Shamsa Sulaiman, Al Blooshi, Ahmad, and Mahmoud Ali Basioni. "Application of Petroleum Geochemistry as a Surveillance Tool for Assessment of Annulus Seepage in Offshore Abu Dhabi, UAE." Paper presented at the Abu Dhabi International Petroleum Exhibition & Conference, Abu Dhabi, UAE, November 2020. doi: https://doi.org/10.2118/203438-MS

Liu, Faye, Wu, Jiang, Jin, Muqing, Hardman, Douglas L., and Dave Cannon. "From Reservoir Characterization to Reservoir Monitoring: An Integrated Workflow to Optimize Field Development Using Geochemical Fingerprinting Technology." Paper presented at the SPE/AAPG/SEG Unconventional Resources Technology Conference, Virtual, July 2020. doi: https://doi.org/10.15530/urtec-2020-2902

McCaffrey, M. A., D. K. Baskin, B. A. Patterson, D. H. Ohms., C. Stone, D. Reisdorf, 2012, Oil fingerprinting dramatically reduces production allocation costs. World Oil, March 2012, p. 55-59.

McCaffrey, Mark A., and David K. Baskin. "Applying Oil Fingerprinting to Unconventional Reservoirs in the Permian Basin for Characterization of Frac Height and Quantification of the Contribution of Multiple Formations to Commingled Production." Paper presented at the SPE/AAPG/SEG Unconventional Resources Technology Conference, San Antonio, Texas, USA, August 2016. doi: https://doi.org/10.15530/URTEC-2016-2460348

McCaffrey, M. A., Legarre H. A. and Johnson S. J. (1996). Using biomarkers to improve heavy oil reservoir management: An example from the Cymric field, Kern County, California. American Association of Petroleum Geologists Bulletin 80(6), p. 904-919.

McCaffrey, M. A., D. H. Ohms., M. Werner, C. Stone, D. K. Baskin, and B. A. Patterson, 2011, Geochemical allocation of commingled oil production or commingled gas production. Society of Petroleum Engineers Paper Number 144618. p 1-19.

McClure, M., C. Kang, S. Medam, C. Hewson, and E. Dontsov. 2022 ResFrac Technical Writeup. [Online]. Available: https://arxiv.org/abs/1804.02092.

Rasdi, Faisal , Salman, Ahmad , Adams, Doyle A., and Zvi Sofer. "An Investigation of Vertical and Lateral Communication in an Unconventional Oil Reservoir Using Geochemistry and Reservoir Simulation." Paper presented at the SPE Canadian Unconventional Resources Conference, Calgary, Alberta, Canada, October 2012. doi: https://doi.org/10.2118/162673-MS

Shahri, Mojtaba , Tucker, Andrew , Rice, Craig , Lathrop, Zach , Ratcliff, Dave , McClure, Mark , and Garrett Fowler. "High Fidelity Fibre-Optic Observations and Resultant Fracture Modeling in Support of Planarity." Paper presented at the SPE Hydraulic Fracturing Technology Conference and Exhibition, Virtual, May 2021. doi: https://doi.org/10.2118/204172-MS

Xing, Lingbo , Teerman, Stan , and Frank Descant. "Time Lapse Production Allocation Using Oil Fingerprinting for Production Optimization in Deepwater Gulf Mexico." Paper presented at the SPE International Conference on Oilfield Chemistry, Galveston, Texas, USA, April 2019. doi: https://doi.org/10.2118/193601-MS